Published in final edited form as:
*J Immunol*. 2014 December 1; 193(11): 5613–5625. doi:10.4049/jimmunol.1401161.

# Compartmentalization of SIV Replication Within Secondary Lymphoid Tissues of Rhesus Macaques is Linked to Disease Stage and Inversely Related to Localization of Virus-Specific CTL1 ,2

**Elizabeth Connick**[*,3], **Joy M. Folkvord**[*], **Katherine T. Lind**[*,†], **Eva G. Rakasz**[‡], **Brodie Miles**[*], **Nancy A. Wilson**[‡,§], **Mario L. Santiago**[*], **Kimberly Schmitt**[¶], **Edward B. Stephens**[¶], **Hyeon O. Kim**[‖], **Reece Wagstaff**[‖], **Shengbin Li**[‖], **Hadia M. Abdelaal**[‖,#], **Nathan Kemp**[‖], **David I. Watkins**[‡,**], **Samantha MaWhinney**[**], and **Pamela J. Skinner**[‖]

[*]Department of Medicine, University of Colorado Anschutz Medical Campus, Denver, CO

[†]Current affiliation, University of Colorado School of Medicine, University of Colorado Anschutz Medical Campus, Denver, CO

[‡] Wisconsin National Primate Research Center, University of Wisconsin-Madison, Madison, WI

[§] Current affiliation, Department of Medicine, Division of Nephrology, University of Wisconsin-Madison, Madison, WI

[¶]Department of Microbiology, Molecular Genetics, and Immunology, University of Kansas Medical Center, Kansas City, KS

[‖]Department of Veterinary and Biomedical Sciences, University of Minnesota, Saint Paul, MN

[**]Current affiliation, Department of Pathology, University of Miami Miller School of Medicine, Miami, FL

[#] Departments of Microbiology and Immunology, Zagazig University, Zagazig, Egypt

[††]Department of Biostatistics and Informatics, University of Colorado Denver, Aurora, CO

## Abstract

We previously demonstrated that HIV replication is concentrated in lymph node B cell follicles during chronic infection and that HIV-specific CTL fail to accumulate in large numbers at those sites. It is unknown whether these observations can be generalized to other secondary lymphoid tissues, or whether virus compartmentalization occurs in the absence of CTL. We evaluated these questions in SIVmac239-infected rhesus macaques by quantifying SIV RNA+ cells and SIV-

[1]This work was supported by Public Health Services Grants from the National Institutes of Health: R01AI096966, R56AI080418, R01AI090795, and the Wisconsin National Primate Research Center (WNPRC) P51OD011106 /P51RR000167 and the WNPRC Pathology and Scientific Protocol Implementation Units, NIH Tetramer Core Facility (contract HHSN272201300006C), NIH Nonhuman Primate Reagent Resource (R24 RR016001, and NIAID contract HHSN 2722000900037C).

[2]These data were presented in part at the19th Conference on Retroviruses and Opportunistic Infections, Seattle, March 5-8, 2012 [abstract 310].

**Corresponding Author:** Elizabeth Connick, M.D. Tel: 303-724-4930; Fax: 303-724-4926; liz.connick@ucdenver.edu.
[3]Address correspondence and reprint requests to: Dr. Elizabeth Connick, Division of Infectious Diseases, University of Colorado Denver, 12700 E 19th Ave, Box B168, Denver, CO 80045.

specific CTL *in situ* in spleen, lymph nodes and intestinal tissues obtained at several stages of infection. During chronic asymptomatic infection prior to simian AIDS (SAIDS), SIV-producing cells were more concentrated in follicular compared to extrafollicular regions of secondary lymphoid tissues. At day 14 of infection, when CTL have minimal impact on virus replication, there was no compartmentalization of SIV-producing cells. Virus compartmentalization was diminished in animals with SAIDS, which often have low frequency CTL responses. SIV-specific CTL were consistently more concentrated within extrafollicular regions of lymph node and spleen in chronically infected animals regardless of epitope specificity. Frequencies of SIV-specific CTL within follicular and extrafollicular compartments predicted SIV RNA+ cells within these compartments in a mixed model. Few SIV-specific CTL expressed the follicular homing molecule CXCR5 in the absence of the extrafollicular retention molecule CCR7, possibly accounting for the paucity of follicular CTL. These findings bolster the hypothesis that B cell follicles are immune privileged sites and suggest that strategies to augment CTL in B cell follicles could lead to improved viral control and possibly a functional cure for HIV infection.

## Introduction

In the absence of antiretroviral therapy, HIV-1 replication continues inexorably and results in progressive depletion of CD4+ T cells, immunodeficiency, and ultimately death of the untreated host. The majority of HIV-1 replication *in vivo* during the chronic phase occurs in secondary lymphoid tissues within CD4+ T cells located in B cell follicles (1-5). SIV replication is also concentrated in CD4+ T cells located primarily in B cell follicles in lymph nodes of chronically infected rhesus macaques (6), which develop a disease similar to HIV-1 infection in humans that progresses to simian AIDS (SAIDS) and death. Mechanisms underlying the compartmentalization of HIV-1 and SIV replication in B cell follicles of lymphoid tissues are not fully understood. Within germinal centers of B cell follicles, the presence of follicular dendritic cells (FDC) laden with extracellular virions (7, 8) that are potently infectious to CD4+ T cells (9) likely plays a significant role in HIV-1 propagation at those sites. Nevertheless, it is unknown why the host immune response is unable to fully suppress HIV-1 replication in the follicular compartment.

CD8+ cytotoxic T cells (CTL) play a key role in control of HIV-1 and SIV replication. CTL develop shortly after primary HIV-1 (10-12) and SIV (13, 14) infection, concurrent with declines in viremia. Diminished HIV-1-specific CTL responses are associated with progression of HIV-1 and SIV infection to AIDS (15, 16) and SAIDS (17), respectively, and are thought to be the result of mutations in CTL epitopes leading to immune escape (18) as well as loss of CD4+ T helper cells that are essential to maintenance of CTL number and function (19, 20). Depletion of CD8+ cells from chronically SIV-infected macaques increases plasma viremia by as much as 1,000-fold (21-23), further supporting the notion that CD8+ T cells exercise substantial antiretroviral activity *in vivo*. Nevertheless, efforts to augment virus-specific CTL through infusion of autologous ex vivo expanded virus-specific CTL (24-27), structured treatment interruption (28), and therapeutic vaccination (29-33) have failed to substantially reduce virus replication. Furthermore, HIV-1 and SIV replication often take place despite high frequencies of HIV-1- and SIV-specific CTL in PBMC. Thus, numerical deficiencies of CTL are not the fundamental cause for ongoing virus replication.

Previously, we demonstrated that virus-specific CTL fail to accumulate in large numbers in B cell follicles in lymph nodes from chronically HIV-1-infected individuals without AIDS (1), and we hypothesized that follicles are immune privileged sites. Limited studies indicate that SIV replication is concentrated in B cell follicles in rhesus macaques during chronic disease (6), and that CTL directed at a Mamu-A1*001:01-restricted Gag epitope (Gag CM9) fail to accumulate in high concentrations in follicles (34). Whether CTL directed at other epitopes also fail to accumulate in large numbers within B cell follicles in chronic SIV infection is unknown. Furthermore, although some studies reported that most virus replication occurs in extrafollicular regions of lymphoid tissues during acute SIV infection (35, 36), the magnitude of virus replication in follicular and extrafollicular compartments has not been quantified in either early or advanced disease. More concrete information on the distribution of virus-producing cells in early lentivirus infection, when the nascent CTL response has had minimal impact on virus replication (37), or in advanced disease, when CTL may be dysfunctional or present at a low frequency, could provide additional insight into the role of CTL in the control of lentivirus replication. To address these questions, we investigated patterns of virus replication and distribution of virus-specific CTL that target multiple SIV epitopes within diverse types of secondary lymphoid tissues of SIV-infected rhesus macaques during acute and chronic SIV infection including some animals with SAIDS. We hypothesized that SIV replication is concentrated in B cell follicles within all secondary lymphoid tissues during chronic disease prior to SAIDS, and that virus-specific CTL directed at multiple SIV epitopes are primarily located in extrafollicular regions of secondary lymphoid tissues, resulting in high *in vivo* virus-specific CTL (effector) to SIV RNA+ (target) cell ratios (E:T) in extrafollicular compartments and low E:T in follicles. We further hypothesized that there is less compartmentalization of virus replication within B cell follicles 14 days after SIV infection, when the newly evolving virus-specific CTL response has had minimal impact on virus replication (37), or during SAIDS, when the CTL response is often attenuated (17).

## Materials and Methods

### Tissue Collection

Lymph nodes, spleen, and intestinal tissues including ileum, cecum, and colon, were obtained from SIVmac239-infected and uninfected Indian rhesus macaques. Axillary and/or inguinal lymph nodes were obtained from all animals. Mesenteric lymph nodes, spleen and intestinal tissues were only obtained from animals at necropsy, which are indicated in Table 1 with the letter “N” appended to the identification number. Five animals (2H2, OH7, 8G5, r03094, and 4440) had samples collected at more than one time point. Twelve animals were inoculated with SIVmac239 intra-rectally, 10 intravenously and one intra-vaginally. Most animals were controls for vaccine studies. Three animals (r01106, RhAU10, RhAX18) were members of an elite controller cohort of rhesus macaques that express the *Mamu-B*008:01* allele (38, 39) and were sacrificed at a time when they were beginning to lose virologic control. Animals were housed and cared for in accordance with American Association for Accreditation of Laboratory Animal Care standards in accredited facilities, and all animal procedures were performed according to protocols approved by the Institutional Animal Care and Use Committees of the Wisconsin National Primate Research Center and the

University of Kansas. Portions of fresh lymphoid tissues were immediately snap frozen in OCT and/or formalin fixed and embedded in paraffin. In animals with MHC class I alleles known to restrict SIV-specific CTL, portions of fresh lymphoid tissue were also collected in RPMI 1640 with sodium heparin (18.7 U/ml) and shipped overnight to the University of Minnesota for *in situ* tetramer staining.

### Localization of SIV RNA+ cells within lymphoid tissues

*In situ* hybridization for SIV RNA was performed using techniques similar to those previously used by us to detect HIV-1 RNA in lymph nodes from humans (2, 40, 41). This technique does not include a protease treatment step to expose encapsulated virion RNA, and as such primarily identifies cells that are actively transcribing SIV. Extracellular virions encapsulated in envelope glycoprotein and bound to FDC are detectable in some instances, but stain faintly in a dendritic conformation that is readily distinguished from the dark blue/black focal staining seen in productively infected cells. Briefly, 6 μm sections of tissue were thaw mounted onto RNase free microscope slides, fixed in 3% paraformaldehyde (Sigma, St. Louis, MO) in diethyl pyrocarbonate (DEPC) (Sigma) treated phosphate buffered saline (PBS), and hybridized with digoxigenin labeled SIVmac239 antisense and sense probes (Lofstrand Laboratories, Gaithersburg, MD), overnight at 50°C. SIV RNA+ cells were visualized using nitro blue tetrazolium/5-bromo- (NBT/BCIP) (Roche, Nutley, NJ), as previously described (2, 40). In some instances, formalin fixed, paraffin embedded (FFPE) tissues were analyzed instead of or in addition to snap frozen tissues. FFPE tissues were mounted onto slides, baked for 1 hour at 60°C, deparaffinized with xylene and rehydrated through graded alcohols to DEPC $H_2O$. FFPE tissues were pre-treated with proteinase K prior to hybridization. In animals for which both snap frozen and FFPE samples were available, similar frequencies of SIV RNA+ cells were detected in both tissues (data not shown). Immunohistochemical staining for B cells was performed in the same tissues using mouse anti-human CD20 (clone 7D1, AbD Serotec, Raleigh, NC), and detected using horse radish peroxidase (HRP) labeled polymer anti-mouse IgG (ImmPress®Kit, Vector Laboratories, Burlingame, CA) and Vector NovaRed substrate (Vector Laboratories). SIV RNA+ cells were counted by visual inspection and classified as either inside or outside of B cell follicles, identified morphologically as a cluster of CD20+ cells, as previously described by us in humans (1, 2). A minimum of 3 sections approximately 30 μm apart were analyzed for each tissue specimen from each animal. Total tissue area and area of follicles was determined by quantitative image analysis (Qwin Pro v3.4.0, Leica, Cambridge, UK) and used to calculate the frequency of SIV+ cells/$mm^2$. A median of 159 $mm^2$ (range 71 – 744 $mm^2$) was evaluated for spleen, 51 $mm^2$ of tissue (range 13 – 442 $mm^2$) for lymph node, 223 $mm^2$ (range, 43-359 $mm^2$) for ileum, 80 $mm^2$ (range, 33 – 212.$mm^2$) for cecum, and 86 $mm^2$ (range, 11 – 164 $mm^2$) for colon.

### Quantification of activated and memory CD4+ cells in lymphoid tissues

Six micron frozen sections of lymph node, spleen and colon tissue from 6 animals were thaw mounted onto slides and fixed in 1% paraformaldehyde. Indirect immunofluorescent staining was performed using rabbit anti-human CD20 (Abcam®, Cambridge, MA), goat anti-CD4 (R&D Systems, Minneapolis, MN), and mouse anti-Ki67 (clone B56, BD Pharmingen) or mouse anti-CD95 (clone DX2, eBiosciences, San Diego, CA) diluted in Tris

Buffered Saline (TBS) with 1% bovine serum albumin (BSA) and incubated for 1 hour. After washing in TBS, secondary antibodies of AF488-labeled anti-goat, AF594-labeled anti-mouse, and AF647-labeled anti-rabbit were added and incubated for 30 min. Slides were covered with coverslips using SlowFade Gold with DAPI (Life Technologies, Grand Island, NY). Images of full sections were generated at 40X using an Olympus VS120 scanner outfitted with an OrcaR2 camera (Olympus, Center Valley, PA). Numbers of CD4+ cells, CD4+Ki67+ or CD4+CD95+ cells within and outside of follicles and their respective areas were determined for each tissue type from ten 40X images (0.02 $mm^2$ each) using Qwin Pro 3.4.0 (Leica Microsystems, Wetzlar, Germany).

### Localization of SIV-specific CTL in lymphoid tissues

*In situ* tetramer staining combined with immunohistochemistry was performed as described previously (1, 42). Briefly, biotinylated MHC class I monomers were loaded with peptides (NIH Tetramer Core Facility) and converted to MHC tetramers. MHC class I monomers used included Mamu-A*001:01 molecules loaded with SIV Gag CM9 (CTPYDINQM) peptides (43), SIV Tat SL8 (STPESANL) peptides (18) or an irrelevant negative control peptides FV10 (FLPSDYFPSV) from the hepatitis B virus core protein; Mamu-B*008:01 molecules loaded with Nef RL10 (RRHRILDIYL) peptides (44), Vif RL9 (RRAIRGEQL) peptides (44), Vif RL8 (RRDNRRGL) peptides (44), and Env KL9 (KRQQELLRL) peptides (44); and Mamu-A1*002:01 monomers loaded with Nef YY9 (YTSGPGIRY) peptides (45). Fresh lymph node and spleen tissues were embedded in low melt agarose and cut using a vibratome into 200 μm thick sections. Ileum was cut with a scalpel into thin strips. Sections were incubated free floating with MHC-tetramers at a concentration of 0.5μg/ml overnight. Sections were then washed, fixed with 4% paraformaldehyde, boiled 3 times in 0.01M urea to expose epitopes, and then permeabilized and blocked with PBS-H containing 0.3% Triton X-100 and 2% normal goat serum for 1 h. For the secondary incubation, sections were incubated with rabbit anti-FITC antibodies (BioDesign, Saco, ME) along with rat-anti-human CD3 antibodies (AbD Serotec clone CD3-12, Raleigh, NC) and mouse-anti-human CD20 antibodies (Novacastra clone L26, Leica Microsystems, Inc., Buffalo Grove, IL) or mouse anti-perforin antibodies (Novacastra) at 4°C on a rocking platform overnight. For the tertiary incubation, sections were washed with PBS-H and incubated with Cy3-conjugated goat-anti-rabbit antibodies (Jackson ImmunoResearch, West Grove, PA), Alexa-488 conjugated goat-anti-mouse antibodies (Molecular probes), and Cy5-conjugated goat-anti-rat antibodies (Jackson ImmunoResearch) or Dylight 649-conjugated goat anti-human IgM (Jackson ImmunoResearch) in blocking solution for 1 to 3 days. For each animal, negative control staining was done that included either the same MHC molecule with irrelevant peptide, a different MHC molecule with irrelevant peptide, or mismatched MHC molecule loaded with SIV peptide. A subset of sections was also stained with mouse-anti-human CD20 antibodies (Novacastra clone L26) and Dylight 649-conjugated goat-anti-human IgM (Jackson ImmunoResearch) to confirm both antibodies colocalized similarly in B cell follicles. Stained sections were imaged using an Olympus FluoView 1000 microscope. Confocal z-series were collected from approximately 5 μm from surface of the tissue section to as deep as the antibody counter-staining penetrated, approximately 35-45 μm into the tissue. Three-dimensional montage images of multiple 800 × 800 pixel 200X Z-scans were created using Olympus FluoView Viewer software.

### Quantification of SIV-specific CTL in situ

Follicular areas were identified morphologically as clusters of brightly stained closely aggregated CD20+ cells. Follicular and extrafollicular areas were delineated using Olympus FluoView FV1000 software. Areas that showed loosely aggregated B cells that were ambiguous as to whether the area was a follicle were not included. To prevent bias, the red tetramer channel was turned off when follicular and extrafollicular areas were delineated. Cell counts were done on single z-scans. While doing the cells counts, we stepped up and down through the z-scans to distinguish tops and bottoms of cells from non-specific background staining and demarcated cells using a software tool to avoid counting the same cell twice. Images were exported as tif files with the area delineations used for cell counting maintained. Image J software was then used to trace and measure the areas delineated for cell counts. An average of 1.4 $mm^2$ (range 0.2 – 5.3 $mm^2$) was evaluated for lymph node and 2 $mm^2$ of tissue (range 0.6 – 4.8 $mm^2$) for spleen.

### Evaluation of CXCR5 expression by indirect immunofluorescent staining

Six micron frozen tissue sections were stained with rabbit anti-CD20 (Abcam®) and mouse anti-rhCXCR5 (NIH Nonhuman Primate Reagent Resource clone 710D82.1) and detected using AF594 anti-rabbit Ig and AF488 anti-mouse Ig (Life Technologies). Images were acquired using a Leica DM5000B fluorescent microscope with appropriate filters.

### Quantification of perforin expressing SIV-specific CTL in situ

Perforin expression within MHC-tetramer-binding cells was determined in confocal images of inguinal and tracheobronchial lymph node sections stained with MHC tetramers[4] (red) and anti-perforin antibodies (green), as well as IgM antibodies (blue) to identify B cell follicles using an Olympus FluoView FV1000 confocal microscope with a 20x objective and 1 μm z-steps. For each section, we collected multiple 800 μm × 800 μm fields and stitched them together to create montage images using Olympus FluoView software. We used FluoView Viewer software to visualize and count tetramer-binding cells that were or were not co-stained with perforin antibodies in follicular and extrafollicular areas. For each sample, an average of 97 (range, 22-300) tetramer+ cells inside follicles and an average of 168 (range, 82-384) tetramer+ cells outside follicles were counted.

### Flow cytometry to detect chemokine receptor and granzyme B expression in SIV-specific CTL

Cryopreserved disaggregated lymphoid tissue cells were thawed, and 1-2 × $10^6$ disaggregated cells were resuspended in 100 μL of tetramer staining buffer (5% fetal bovine serum in PBS with 0.06% sodium azide) and incubated with APC-labeled Gag CM9 tetramer (MBL International, Woburn, MA), APC-labeled Nef RL10 tetramer (NIH Tetramer Core Facility, Emory University, Atlanta, GA), or BV421-labelled Nef YY9 tetramer (NIH Tetramer Core Facility) concurrently with CXCR5-PE (eBioscience clone MU5UBEE), CD8-eFlour605 (eBioscience clone RPA-T8), CCR7-FITC (R&D Systems clone 150503), CD3-APC Cy7 (BD clone SP34-2) and Aqua Live/Dead viability marker (Life Technologies L34957) in the dark for 40 minutes at room temperature. Cells were washed twice, fixed and permeabilized at 4°C for 20 minutes (BD 55028), washed again,

and stained with granzyme B-PE Cy5.5 (Invitrogen clone GB11) at 4°C for 30 minutes. After washing twice, the cells were resuspended and data were acquired on a LSRII flow cytometer (Becton Dickinson Immunocytometry Systems, San Jose, CA) and analyzed using FlowJo (Treestar, Tree Star, Ashland, OR).

### Statistical Analysis

Hypothesis tests were assumed to be two-sided with a significance level of 0.05. To control type-I error, a Fisher's least protected approach was used for comparisons over tissue types (lymph node, intestine, and spleen). Mixed effects models were used to accommodate repeated measures on each animal with $\log_{10}$ transformations to normalize outcomes prior to analysis. Model estimates were back-transformed for interpretation (geometric mean approach). Count and area data from multiple sections were summed and SIV RNA+ cells/$mm^2$ calculated. Count data were analyzed using a generalized linear model for a negative binomial distribution that accounted for within subjects correlation and adjusted for $\log_e$ (area). If more than one lymph node was analyzed from a specific site obtained on the same date, data were reported as an average of all lymph node data from that site. For analyses of follicular and extrafollicular concentrations of SIV RNA+ cells, results were excluded if the total number of SIV RNA+ cells observed was less than 5. A minimum of 3 follicles were required to be observed when quantifying tetramer+ cells in tissues. Comparing frequency of tetramer+ SIV-specific CTL between extrafollicular vs. follicular regions, findings were collapsed by animal (all F<E) and an exact binomial test was utilized to calculate a maximum p-value. SAS (version 9.3, Cary NC), R version 2.13.2 and GraphPad Prism (6.0) software were utilized.

## Results

### Rhesus macaque clinical characteristics

Secondary lymphoid tissue specimens from 6 acutely SIV-infected macaques, 14 chronically infected macaques without SAIDS, and 9 chronically infected macaques with SAIDS were evaluated. Clinical and experimental characteristics of these animals are shown in Table I. Acutely infected macaques had lymph nodes collected 14 days after infection; they had a median plasma SIV RNA viral load of 8.98 $\log_{10}$ copies/mL and a median CD4+ T cell count of 1,063 cells/$mm^3$. Chronically infected animals without SAIDS were infected for a median of 22 weeks; they had a median viral load of 5.81 $\log_{10}$ copies/mL and a median CD4+ T cell count of 368 cells/$mm^3$. Seven of the 9 animals with SAIDS had a CD4+ T cell count less than 200 cells/$mm^3$. The other two animals had CD4+ T cell counts above 200 cells/$mm^3$, but were sacrificed due to development of conditions associated with SAIDS to prevent suffering. Animals with SAIDS were infected a median of 26 weeks, had a median viral load of 6.2 $\log_{10}$ copies/mL, and a median CD4+ T cell count of 142 cells/$mm^3$.

### Distribution of SIV RNA+ cells in secondary lymphoid tissues during chronic asymptomatic SIV infection

SIV RNA+ cells were detected by *in situ* hybridization in all secondary lymphoid tissue samples from chronically infected animals without SAIDS, as shown in representative images in Figure 1. Tissues from uninfected animals that were stained with anti-sense

probes and tissues from SIV-infected animals that were stained with sense probes were uniformly negative (data not shown). Within the same tissue type, i.e., lymph node or intestine, frequencies of SIV RNA+ cells were similar ($p = 0.754$) (Figure 2A). Frequencies of SIV RNA+ cells in spleen tended to be lower than those in lymph node, although differences were not statistically significant. Frequencies of SIV RNA+ cells were approximately six- and ten-fold lower in intestinal tissues compared to spleen ($p<0.0001$) and lymph node ($p<0.0001$), respectively.

SIV RNA+ cells were significantly more concentrated in B cell follicles compared to extrafollicular regions for all tissue types (Figure 2B). This pattern was consistent among all animals with one exception (R02076-N). This animal (indicated in closed circles in Figure 2B) demonstrated similar frequencies of SIV RNA+ cells in follicular and extrafollicular regions in axillary and mesenteric lymph nodes, but higher frequencies within follicles compared to extrafollicular tissues in spleen, inguinal lymph node and intestine. Of note, this animal had one of the lowest CD4+ T cell counts of all the chronically infected, asymptomatic macaques.

Follicular:extrafollicular ratio of SIV RNA+ cells was marginally higher in spleen (geometric mean, 7.1) compared to lymph node (geometric mean, 3.1; $p=0.0005$), but was substantially higher in intestinal tissues (geometric mean, 32.0) compared to both lymph node ($p<0.0001$) and spleen ($p<0.0001$) (Figure 2B). Differences between intestine and other tissues were largely driven by differences in frequencies of SIV RNA+ cells in extrafollicular regions; there were substantially fewer SIV RNA+ cells in extrafollicular regions of intestinal tissues (geometric mean, 0.16 cells/$mm^2$, 95% CI 0.081, 0.32) compared to spleen (geometric mean 0.45 cells/$mm^2$, 95% CI 0.21, 0.98; $p<0.0019$) and lymph nodes (geometric mean 1.3 cells/$mm^2$, 95% CI 0.68, 2.5; $p<0.0001$). Frequencies of SIV RNA+ cells in follicles, on the other hand, were not statistically different among the tissue types ($p=0.32$) ranging from a geometric mean of 3.2 cells/$mm^2$ (95% CI 1.5, 7.0) in spleen to 3.9 cells/$mm^2$ (95% CI 2.0, 7.6) in lymph node and 5.1 cells/$mm^2$ (95% CI 2.5, 10.2) in intestine. Overall, only a small fraction (geometric mean, 2.8%) of the intestinal tissues consisted of follicles, which was significantly lower than that in spleen (28%) and lymph nodes (40%) (Figure 2C). The majority of SIV RNA+ cells were found within follicles in both spleen and lymph nodes, whereas a geometric mean of 40% of SIV RNA+ cells was found in follicles in intestine (Figure 2D). Interestingly, most SIV RNA+ cells observed in extrafollicular regions of intestinal tissues were located close to a B cell follicle (e.g., Figures 1E and 1F).

To evaluate whether differences in frequencies of virus-producing cells between follicular and extrafollicular regions or among tissues could be related to target cell availability, frequencies of CD4+ cells, CD95+ (memory) CD4+ cells, and Ki67+ (activated) CD4+ cells were determined within spleen, lymph node, and colon of six animals (Supplemental Figure 1). Significant differences in frequencies of CD4+ cells and CD95+CD4+ cells were observed between follicular and extrafollicular regions of secondary lymphoid tissues, although the differences varied by tissue ($p<0.0001$); CD4+ cells and CD95+CD4+ cells were significantly more abundant in follicles compared to extrafollicular regions of spleen (F:EF 1.5 for both; $p=0.01$ and 0.02, respectively) and colon (3.0 and 2.8, respectively;

p<0.001 for both), whereas they were significantly less abundant in follicles of lymph nodes compared to extrafollicular tissues (F:EF 0.6 for both; p=0.01 and 0.007, respectively) (Supplemental Figure 1A, 1B). Ki67+CD4+ cells, on the other hand, were more abundant in follicular compared to extrafollicular regions of all tissues (F:EF 1.5; p<0.003), and the relationship did not differ across tissues (p=0.10) (Supplemental Figure 1C). Frequencies of SIV RNA+ cells remained consistently higher within the follicular compartment compared to the extrafollicular compartment in all tissues, after adjusting for CD4+ cells (F:EF 6.3, 95% CI 3.3, 12.0; p<0.0001), memory CD4+ cells (F:EF 6.6, 95% CI, 3.5, 12.4; p<0.0001; Figure 2E), or Ki67+CD4+ cells (F:EF 6.2, 95% CI, 3.2, 12.1; p<0.0001). There were no statistically significant differences in the F:EF ratio of virus-producing cells across spleen, lymph node, and colon after adjusting for frequencies of CD4+ cells (p=0.78), CD95+CD4+ cells (p=0.67; Figure 2E), or Ki67+CD4+ cells (p=0.55).

## Distribution of SIV RNA+ cells in lymph nodes of SIV-infected macaques during acute SIV infection and SAIDS

Frequencies of SIV RNA+ cells were significantly lower in lymph nodes from chronically infected animals compared to those from animals 14 days after infection and tended to be lower compared to those from animals with SAIDS (Figure 3A). No evidence of compartmentalization of SIV RNA+ cells within B cell follicles was observed in any of the acutely infected animals, in marked contrast to findings seen in animals with chronic infection (Figure 3B). In animals with SAIDS, some demonstrated a follicular concentration of SIV RNA+ cells in lymph nodes, whereas others did not, and overall concentrations of SIV RNA+ cells were not statistically different between the two compartments (Figure 3B). The follicular to extrafollicular ratio of SIV RNA+ cells was significantly higher in chronically infected animals compared to those with acute SIV infection (p=0.0004) and tended to be higher compared to those with SAIDS (p=0.18) (Figure 3B). The percentage of tissue that consisted of follicle did not differ significantly among animals by disease stage (Figure 3C). Percentages of SIV RNA+ cells that resided in follicles, however, were significantly higher in animals with chronic infection compared to those with acute infection (p=0.02), and tended to be higher compared to those with SAIDS (Figure 3D). When data from animals at all stages of disease were combined, frequencies of SIV RNA+ cells predicted plasma viral load (Figure 3E). In an analysis that included all animals, the $\log_{10}$ follicular:extrafollicular ratio of SIV RNA+ cells in lymph nodes predicted $\log_{10}$ plasma viral load (Figure 3F). Notably, the two animals with the highest degree of compartmentalization, i.e., the highest $\log_{10}$ follicular: extrafollicular ratio in Figure 3F, were both chronically infected animals that expressed the *Mamu-B*008:01* MHC allele.

## Distribution of SIV-specific CTL in secondary lymphoid tissues during chronic SIV infection

CTL directed at 7 different SIV epitopes and restricted by 3 different MHC class I molecules were identified by *in situ* MHC class I tetramer binding in secondary lymphoid tissues from 8 animals with chronic SIV infection including SAIDS (Supplemental Table I). When SIV-specific CTL were detected at high frequencies in one tissue from an animal, they were also detected in other tissues examined from that animal (Supplemental Table I). Frequencies of SIV-specific CTL were quantified in 23 lymph nodes from 8 animals and ranged from 10 to

522 cells/ $mm^2$. SIV-specific CTL were also quantified in spleens of 6 of these animals and ranged from 22 to 327 cells/ $mm^2$. Frequencies of SIV-specific CTL did not differ significantly between lymph nodes and spleen (p=0.44).

SIV-specific CTL were generally distributed diffusely amongst other CD8+ T cells and in all animals were consistently more concentrated in the extrafollicular regions in both lymph node and spleen compared to follicular regions regardless of the MHC class I type of the animal or the SIV epitope presented by the tetramer (Figure 4A). The highest frequencies of both follicular and extrafollicular SIV-specific CTL were found in the 3 animals that expressed the *Mamu-B*008:01* MHC allele. In all animals, there was a range of localization patterns of SIV-specific CTL within follicles (Figure 5A-D). In most instances, SIV-specific CTL were largely absent from the follicles, as illustrated in Figure 5B and 5C. When SIV-specific CTL were found in B cell follicles, typically they were located near the edge of the follicles (Figure 5C), although in some instances they were located throughout the follicle cross-section (Figure 5D). Scanning through three dimensions within B cell follicles revealed that in most follicles there were large contiguous areas that were completely devoid of SIV-specific CTL. The frequency of virus-specific CTL in the extrafollicular region was predictive of the frequency in the follicular region (4B). The median ratio of extrafollicular to follicular SIV-specific CTL in both lymph node and spleen was 4 (Figure 4C). There was no obvious difference in the extrafollicular to follicular ratios of SIV-specific CTL related to MHC class I allele expression or the SIV epitope targeted, although the numbers of animals studied was too small to exclude the possibility that such a difference exists.

In intestinal tissues, *in situ* tetramer staining analysis was limited to the ileum from two chronically infected animals (Rhau10, Rhax18), and one animal with SAIDS (R01106) and results were not quantified due to limited numbers of follicles detected in tissue sections. Rhau10 demonstrated a few B*008:01/Vif RL9- and Nef RL10-specific CTL (Supplemental Figure 2A) that were localized exclusively in extrafollicular regions. Rhax18 demonstrated a few B*008:01/Nef RL10-specific CTL scattered in the extrafollicular regions, and a larger number around and inside the one follicle that was observed (Supplemental Figure 2B). In the animal with SAIDS, R01106, B*008:01/Env KL9-specific CD8+ T cells (Supplemental Figure 2C) were detected at higher levels than in the other two animals. In this animal, more abundant extrafollicular CTL were observed than in the other two animals and, similar to Rhax18, large concentrations of CTL were found around and inside the B cell follicles.

## Effector SIV-specific CTL to SIV RNA+ target cell (E:T) ratios in secondary lymphoid tissues

The *in vivo* E:T ratios between the dominant, i.e., most abundant SIV-specific CTL and SIV RNA+ cells ranged from 2 to 235 (median, 36) in lymph node and 6 to 7,509 (median, 69) in spleen. The E:T ratio did not correlate with plasma viral load in either lymph node (r=−0.5; p=0.207; 95% CI −0.89, 0.31) or spleen (r=−0.371; p=0.468; 95% CI −0.91, 0.63), although the number of animals studied was small and this does not exclude a relationship. Notably, the three animals with the lowest *in vivo* E:T ratios had the highest viral loads (Rh2306, R03094, R03111). When *in vivo* E:T ratios were analyzed within lymphoid follicular and extrafollicular compartments using the dominant SIV-specific CTL, significantly higher

ratios were found in extrafollicular tissues of both lymph node (median, 127) and spleen (median, 375) compared to follicular tissues (lymph node median, 3; spleen median, 9) (Figure 6A).

Frequencies of the dominant virus-specific CTL, without regard to compartment, were not predictive of plasma viral load for either lymph node (r=−0.07; 95% CI, −0.74, 0.67; p=0.87) or spleen (r=−0.31; 95% CI, −0.90, 0.67; p=0.544). However in a mixed model, combining data from both lymph node and spleen, $\log_{10}$ frequencies of CTL were inversely related to $\log_{10}$ frequencies of SIV RNA+ cells in the tissue. On average, for every one log increase in CTL there was a 0.81 $\log_{10}$ decrease (95% CI −1.82, 0.20)in SIV RNA+ cells (p=0.089). Interestingly, when frequencies of CTL in follicular and extrafollicular compartments were evaluated together vis-a-vis SIV RNA+ cells in those compartments, there was a significant inverse relationship (Figure 6B).

## Expression of CXCR5 and CCR7 on virus-specific CTL

It is well established that upregulation of CXCR5 and downregulation of CCR7 are required to enable the follicular subset of CD4+ T cells to migrate into B cell follicles (46). Assuming that a similar mechanism promotes CD8+ T cell migration into B cell follicles, we hypothesized that absence of CXCR5 and/or presence of CCR7 on SIV-specific CTL might account for low frequencies of these cells in B cell follicles. We first evaluated the distribution of CXCR5 in lymph nodes (n=5) and spleens (n=2) from chronically SIV-infected rhesus macaques. We found that the majority of CXCR5+ cells were localized within B cell follicles, as shown in representative images in Figures 7A and 7B, confirming that the expected localization of CXCR5-expressing cells in B cell follicles exists in SIV infection. We next evaluated CXCR5 and CCR7 expression on virus-specific CTL using cryopreserved, disaggregated cells from spleen and lymph nodes that were stained with antibodies and MHC class I tetramers, and analyzed by flow cytometry (Supplemental Figure 3). CXCR5+CCR7- SIV-specific CTL were a minority population in all animals and all tissues; while the CXCR5-CCR7+ and CXCR5-CCR7- CTL subsets were the most abundant (Figure 7C).

## Expression of CTL effector molecules by virus-specific CTL

To evaluate whether CTL dysfunction might hinder clearance of SIV-producing cells within B cell follicles, granzyme B and perforin expression were determined on SIV-specific CTL. Using disaggregated cells from the same animals as those in Figure 7E, we determined granzyme B staining within each chemokine receptor expressing CTL subset by flow cytometry (Supplemental Figure 3). As shown in Figure 8A, CXCR5 expression correlated with the most granzyme-expressing cells, regardless of whether they expressed CCR7, whereas low levels of granzyme B were observed in CXCR5- subsets. Perforin expression was evaluated by immunofluorescent staining within virus-specific CTL identified through *in situ* tetramer staining. As shown in Figures 8B and 8C, perforin+ and perforin- SIV-specific CTL were observed within both follicular and extrafollicular regions of tissues, respectively. Perforin expression was 15.9% lower within the follicular population of SIV-specific CTL compared to CTL in the extrafollicular region (Figure 8D).

## Discussion

This is the first study to quantify and compare the distribution of virus replication within multiple secondary lymphoid tissues during chronic SIV disease, as well as during acute infection and SAIDS. This is also the first study to quantify diverse virus-specific CTL within follicular and extrafollicular compartments of secondary lymphoid tissues during chronic disease. We found that virus replication was concentrated in B cell follicles in all secondary lymphoid tissues of chronically infected rhesus macaques prior to SAIDS even after adjusting for differences in frequencies of viral target cells, demonstrating that compartmentalization of SIV replication is a widespread phenomenon. In contrast, the follicular concentration of SIV replication was uniformly absent in animals at day 14 of SIV infection, when the nascent CTL response has had minimal impact on virus replication (13, 14). Furthermore, compartmentalization of SIV replication was attenuated or lost in animals with SAIDS, when SIV-infected macaques often have substantial reductions in CTL and impairments in CTL function (17). SIV-specific CTL were distributed in a pattern inverse to that of SIV RNA+ cells, with high concentrations of virus-specific CTL in extrafollicular regions and low concentrations in B cell follicles during chronic disease. Effector (CTL) to target (SIV RNA+) cell ratios in spleen and lymph node were on average more than 40-fold higher in extrafollicular regions compared to B cell follicles. Frequencies of virus-specific CTL within follicular and extrafollicular compartments predicted frequencies of virus-producing cells within those sites when analyzed together, providing additional evidence that *in vivo* levels of CTL are significant determinants of virus replication. Collectively, these data suggest that virus-specific CTL are highly efficient at suppressing lentivirus replication in extrafollicular tissues during chronic, asymptomatic disease because they are present in those tissues in large numbers, but that they are unable to suppress virus replication within follicles due to low frequencies at those sites. These findings further bolster our hypothesis that B cell follicles are immune privileged sites due to the fact that CTL fail to accumulate in large numbers in that compartment, thereby establishing a reservoir of chronic lentivirus replication (1, 2).

This study is the first to directly compare frequencies of virus-producing cells among secondary lymphoid tissues during chronic infection. Importantly, we quantified virus-producing cells using a technique that readily distinguishes between virus-producing cells and virions bound extracellularly to FDC, because the latter would not be targeted by CTL as they are not productively infected (47) and consequently do not present antigen in the context of MHC class I molecules required for CD8+ T cell recognition. Although the phenotype of SIV RNA+ cells was not determined in this study, previous studies have demonstrated that the majority of SIV-producing cells in secondary lymphoid tissues of rhesus macaques are CD4+ T cells (48, 49). Overall, frequencies of SIV RNA+ cells were 6-fold lower in intestinal tissues compared to spleen and 10-fold lower compared to lymph node (Figure 2A). In light of estimates that intestine contains approximately 10 times more tissue than spleen (50), these data suggest that intestine harbors approximately 1.7 times more virus-producing cells *in vivo* than spleen, an organ which has generally been considered to harbor a minor portion of replicating virus. Recent studies have challenged the notion that intestinal tissues harbor the majority of CD4+ T cells *in vivo* (50, 51), which has

been the primary basis for assertions that the majority of HIV-1 and SIV replication occurs in the gut. Furthermore, phylogenetic studies of virus in SIV-infected rhesus macaques indicate that gut is not the major source of plasma virus *in vivo* (52, 53), and one study suggested that lymph nodes are the major source (54). Collectively, these data suggest that the intestine is a minor source of plasma virus during chronic, asymptomatic disease. Further studies to precisely quantify the amount of virus-producing cells in secondary lymphoid tissues by measuring the dimensions of the tissues could be useful in establishing the true contribution of each tissue type to virus production during both acute and chronic infection.

Similar levels of virus replication were seen in B cell follicles in spleen, lymph nodes, and intestinal tissues during chronic infection, suggesting that the factors that promote SIV replication within follicles are consistent across these diverse tissue environments. Location of the virus-producing cells within B cell follicles is highly suggestive that these cells are T follicular helper cells, but further studies to clarify the phenotype of these virus-producing cells are warranted. Marked differences in virus replication were found among extrafollicular regions of secondary lymphoid tissues; frequencies of SIV RNA+ cells in the lamina propria of intestine were on average 10- to 14-fold lower than those in the extrafollicular regions of spleen and lymph node, respectively. These differences appeared to be largely explained by lower concentrations of memory CD4+ cells in lamina propria compared to extrafollicular regions of spleen and lymph node, as differences in virus-producing cells in the extrafollicular compartment disappeared after adjusting for frequencies of memory CD4+ cells. Relatively low numbers of memory CD4+ cells in the lamina propria of the intestine may exist due to either intrinsic differences among the tissues (50, 51) or selective loss during acute SIV infection (55). Importantly, there was no evidence from our studies of a more robust CTL response in the lamina propria of the ileum compared to extrafollicular regions of lymph nodes and spleen to account for fewer virus-producing cells in the lamina propria of the intestine . The observation that SIV RNA+ cells in the lamina propria of intestinal tissues were usually located near B cell follicles raises the interesting possibility that virus-producing cells in the lamina propria are cells that recently emigrated from follicles, possibly after being infected through interactions with FDC. Indeed, a major difference between the intestinal tissues and the spleen and lymph node was the relative paucity of follicles in the intestine, which could account for the relatively lower level of SIV replication in the lamina propria if most virus-producing cells originate in follicles. It is possible that most SIV RNA+ cells originate in follicles in lymph nodes and spleen as well, but because of the close adjacency of follicles in those tissues a gradient in distribution of extrafollicular virus-producing cells vis-a-vis the follicles is less readily observed.

The magnitude of compartmentalization of SIV RNA+ cells in lymph nodes, as signified by the follicular to extrafollicular (F:EF) ratio, was strongly related to plasma viral load (Figure 3E). This was true not only for animals with chronic infection, but also those with acute infection and SAIDS. Compartmentalization of virus replication within B cell follicles has been associated with a beneficial phenotype in rhesus macaques infected with *nef*-deleted SIVmac239. In these animals, which usually have very low viral loads and a non-progressor phenotype, almost all virus-producing cells are found within B-cell follicles in secondary

lymphoid tissues (56). Mechanisms underlying the profound compartmentalization of virus replication in this model are not clear, but could include enhanced CTL killing of virus-producing cells in extrafollicular tissues due to abrogation of Nef-induced downregulation of MHC class I molecules (57). Intriguingly, and in contrast to the rhesus macaque model, the non-progressive phenotype seen in SIV-infected sooty mangabeys is not associated with compartmentalization of virus replication (6). Indeed, these animals, which fail to progress to SAIDS despite high viral loads, demonstrate neither a follicular concentration of virus replication nor large numbers of virions associated with FDC (6). Reasons for this distinct distribution of virus-producing cells in sooty mangabeys are unclear but could include lack of permissiveness of T follicular helper cells to SIV, failure of FDC to bind virion antibody complexes, or presence of high concentrations of CTL in the follicular microenvironment. The failure of sooty mangabeys to develop progressive disease has been attributed to lack of infection of central memory cells (6). It should be noted, however, that frequencies of virus-producing cells in lymph nodes of these animals were substantially lower than those in SIV-infected rhesus macaques (6), which could provide an alternative explanation for their relatively delayed disease progression. Regardless, these findings suggest that mechanisms that underlie non-progressive SIV disease in sooty mangabeys may be fundamentally different from those in rhesus macaques.

In the present study, the lack of compartmentalization of virus replication during early SIV infection and diminished compartmentalization during SAIDS were interpreted as evidence that CTL are essential to compartmentalization of virus in B cell follicles. Alternative explanations should nevertheless be considered. It is possible that a highly vulnerable target cell population in the extrafollicular region is preferentially infected and destroyed during acute SIV infection, resulting in compartmentalization of virus in the B cell follicles in chronic disease due to loss of extrafollicular target cells. Nevertheless, a follicular concentration of virus replication was found even after adjusting for frequencies of total CD4+ cells, memory CD4+ cells or Ki67+ CD4+ cells, weighing against this explanation. In addition, the fact that virus replication in the extrafollicular regions was elevated in some animals with SAIDS and associated with loss of compartmentalization (Figure 3B) further argues against a theory of limited target cells in extrafollicular regions. Nevertheless, a change in virus coreceptor usage could have increased the permissiveness of target cells in the extrafollicular region, causing this loss of compartmentalization in some animals with advanced disease. Studies of virus coreceptor tropism or deep sequencing of the virus envelope to evaluate for mutations in these animals could be useful in excluding this possibility. Furthermore, studies of the effects of CD8 depletion on chronically infected macaques could further address the question of whether the extrafollicular target cell population is depleted or if virus replication is suppressed by CTL.

The findings that virus-specific CTL failed to accumulate in large numbers in B cell follicles in both spleen and lymph node during chronic SIV infection confirmed our previous observations in humans (1) as well as one previous description of Mamu-A1*001:01/Gag-specific CD8 T cells in 3 SIV-infected rhesus macaques (34). The novelty of the present study is that this pattern was evident for multiple different SIV epitopes presented by several different MHC class I molecules, indicating that this is a generalized phenomenon of SIV-specific CTL and not unique to a few animals, MHC types, or epitopes. Importantly, few

SIV-specific CTL expressed the follicular homing molecule CXCR5 in the absence of the extrafollicular retention molecule CCR7, which may account for the paucity of CTL in follicles. It would be important to determine in future studies whether there are differences in the degree of follicular localization of CTL or their expression of CXCR5 and CCR7 related to MHC restricting molecule or SIV epitope targeted, as the present study had insufficient numbers of animals to address these questions. B*008:01 animals in our study demonstrated the largest virus-specific CTL responses as well as the highest degree of compartmentalization of virus replication. These animals had been previously elite controllers, and were beginning to lose virologic control at the time that they were studied. It would be important in future studies to determine whether B*008:01 animals with intact elite control demonstrate more compartmentalization as well as higher frequencies of extrafollicular CTL than B*008:01 animals that do not achieve virologic control, or B*008:01 animals that have completely lost virologic control.

Studies to evaluate whether follicular CTL have impairments in effector function were equivocal. Higher percentages of granzyme B+ cells were found in CXCR5+CTL including the CCR7- subset, which is presumably representative of follicular CTL. On the other hand, *in situ* studies demonstrated approximately 16% fewer follicular CTL expressed perforin compared to extrafollicular CTL, suggesting a possible subtle impairment in effector function in follicular virus-specific CTL in addition to numerical impairments. Further studies to evaluate the ability of follicular SIV-specific CTL to suppress virus replication compared to extrafollicular CTL are warranted to definitively address this question, as phenotypic studies do not necessarily fully reflect effector function. Such studies would require virus-specific CTL to be sorted prior to assay, as CXCR5 is transiently upregulated on CTL after antigen-specific stimulation [(58) and unpublished observations], which would confound results if CXCR5 is also used to identify follicular CTL. Additional factors, such as T regulatory cells, may also be affecting virus-specific CTL proliferation and function within and outside of the follicles (59), and are worthy of further investigation.

The present study has provided strong circumstantial evidence that B cell follicles are immune privileged sites where SIV-specific CTL that target multiple different epitopes fail to accumulate, thereby allowing virus replication to persist during chronic asymptomatic disease. Additional studies demonstrating that introduction of virus-specific CTL into follicles suppresses lentivirus replication at those sites would be necessary to provide conclusive evidence that a deficiency of CTL in follicles accounts for chronic lentivirus replication at those sites. It is possible that delivering CTL to follicles may not be sufficient to suppress virus replication. For example, germinal center B cells express high levels of PD-L1 in HIV-1 infection (60), which is known to inhibit CTL activity (61). Whether this would be functionally relevant *in vivo* is not clear. A recent study linked the magnitude of the cellular immune response in lymphoid tissues with protection from pathogenic infection in rhesus macaques vaccinated with a live-attenuated SIV that induces CTL (62). Whether CTL in these protected animals entered the follicles, however, is unknown. A better understanding of the immunologic and virologic milieu in B cell follicles during lentivirus infection and in the context of vaccination is essential to the development of effective preventive and therapeutic strategies for HIV-1 infection.

## Supplementary Material

Refer to Web version on PubMed Central for supplementary material.

## Acknowledgments

We would like to thank Emily Thompson, Rafael Barbosa, Nik Kinzel, and Teresa Mattila for assistance with confocal imaging and quantitative image analysis of *in situ* tetramer stained sections, the Immunology Services and Virology Services units at the Wisconsin National Primate Research Center for providing CD4 count and plasma viral load data; Heather Simmons of the Wisconsin National Primate Center for consultation and assistance in providing rhesus macaque tissue specimens; and Dennis Burton and Ashley Haase for sharing of rhesus macaque lymphoid tissues.

## References

1. Connick E, Mattila T, Folkvord JM, Schlichtemeier R, Meditz AL, Ray MG, McCarter MD, Mawhinney S, Hage A, White C, Skinner PJ. CTL fail to accumulate at sites of HIV-1 replication in lymphoid tissue. J Immunol. 2007; 178:6975–6983. [PubMed: 17513747]
2. Folkvord JM, Armon C, Connick E. Lymphoid follicles are sites of heightened human immunodeficiency virus type 1 (HIV-1) replication and reduced antiretroviral effector mechanisms. AIDS Res Hum Retroviruses. 2005; 21:363–370. [PubMed: 15929698]
3. Hufert FT, van Lunzen J, Janossy G, Bertram S, Schmitz J, Haller O, Racz P, von Laer D. Germinal centre CD4+ T cells are an important site of HIV replication in vivo. Aids. 1997; 11:849–857. [PubMed: 9189209]
4. Tenner-Racz K, Stellbrink HJ, van Lunzen J, Schneider C, Jacobs JP, Raschdorff B, Grosschupff G, Steinman RM, Racz P. The unenlarged lymph nodes of HIV-1-infected, asymptomatic patients with high CD4 T cell counts are sites for virus replication and CD4 T cell proliferation. The impact of highly active antiretroviral therapy. J Exp Med. 1998; 187:949–959. [PubMed: 9500797]
5. Biberfeld P, Chayt KJ, Marselle LM, Biberfeld G, Gallo RC, Harper ME. HTLV-III expression in infected lymph nodes and relevance to pathogenesis of lymphadenopathy. Am J Pathol. 1986; 125:436–442. [PubMed: 3642987]
6. Brenchley JM, Vinton C, Tabb B, Hao XP, Connick E, Paiardini M, Lifson JD, Silvestri G, Estes JD. Differential infection patterns of CD4+ T cells and lymphoid tissue viral burden distinguish progressive and nonprogressive lentiviral infections. Blood. 2012; 120:4172–4181. [PubMed: 22990012]
7. Embretson J, Zupancic M, Ribas JL, Burke A, Racz P, Tenner-Racz K, Haase AT. Massive covert infection of helper T lymphocytes and macrophages by HIV during the incubation period of AIDS. Nature. 1993; 362:359–362. [PubMed: 8096068]
8. Pantaleo G, Graziosi C, Demarest JF, Butini L, Montroni M, Fox CH, Orenstein JM, Kotler DP, Fauci AS. HIV infection is active and progressive in lymphoid tissue during the clinically latent stage of disease. Nature. 1993; 362:355–358. [PubMed: 8455722]
9. Heath SL, Tew JG, Szakal AK, Burton GF. Follicular dendritic cells and human immunodeficiency virus infectivity. Nature. 1995; 377:740–744. [PubMed: 7477265]
10. Borrow P, Lewicki H, Hahn BH, Shaw GM, Oldstone MB. Virus-specific CD8+ cytotoxic T-lymphocyte activity associated with control of viremia in primary human immunodeficiency virus type 1 infection. J Virol. 1994; 68:6103–6110. [PubMed: 8057491]
11. Connick E, Marr DG, Zhang XQ, Clark SJ, Saag MS, Schooley RT, Curiel TJ. HIV-specific cellular and humoral immune responses in primary HIV infection. AIDS Res Hum Retroviruses. 1996; 12:1129–1140. [PubMed: 8844017]
12. Koup RA, Safrit JT, Cao Y, Andrews CA, McLeod G, Borkowsky W, Farthing C, Ho DD. Temporal association of cellular immune responses with the initial control of viremia in primary human immunodeficiency virus type 1 syndrome. J Virol. 1994; 68:4650–4655. [PubMed: 8207839]
13. Kuroda MJ, Schmitz JE, Charini WA, Nickerson CE, Lifton MA, Lord CI, Forman MA, Letvin NL. Emergence of CTL coincides with clearance of virus during primary simian

immunodeficiency virus infection in rhesus monkeys. J Immunol. 1999; 162:5127–5133. [PubMed: 10227983]

14. Yasutomi Y, Reimann KA, Lord CI, Miller MD, Letvin NL. Simian immunodeficiency virus-specific CD8+ lymphocyte response in acutely infected rhesus monkeys. J Virol. 1993; 67:1707–1711. [PubMed: 8437240]
15. Klein MR, van Baalen CA, Holwerda AM, Kerkhof Garde SR, Bende RJ, Keet IP, Eeftinck-Schattenkerk JK, Osterhaus AD, Schuitemaker H, Miedema F. Kinetics of Gag-specific cytotoxic T lymphocyte responses during the clinical course of HIV-1 infection: a longitudinal analysis of rapid progressors and long-term asymptomatics. J Exp Med. 1995; 181:1365–1372. [PubMed: 7699324]
16. Hoffenbach A, Langlade-Demoyen P, Dadaglio G, Vilmer E, Michel F, Mayaud C, Autran B, Plata F. Unusually high frequencies of HIV-specific cytotoxic T lymphocytes in humans. J Immunol. 1989; 142:452–462. [PubMed: 2463308]
17. Villada IB, Mortara L, Aubertin AM, Gras-Masse H, Levy JP, Guillet JG. Positive role of macaque cytotoxic T lymphocytes during SIV infection: decrease of cellular viremia and increase of asymptomatic clinical period. FEMS immunology and medical microbiology. 1997; 19:81–87. [PubMed: 9322072]
18. Allen TM, O'Connor DH, Jing P, Dzuris JL, Mothe BR, Vogel TU, Dunphy E, Liebl ME, Emerson C, Wilson N, Kunstman KJ, Wang X, Allison DB, Hughes AL, Desrosiers RC, Altman JD, Wolinsky SM, Sette A, Watkins DI. Tat-specific cytotoxic T lymphocytes select for SIV escape variants during resolution of primary viraemia. Nature. 2000; 407:386–390. [PubMed: 11014195]
19. Janssen EM, Lemmens EE, Wolfe T, Christen U, von Herrath MG, Schoenberger SP. CD4+ T cells are required for secondary expansion and memory in CD8+ T lymphocytes. Nature. 2003; 421:852–856. [PubMed: 12594515]
20. Vaccari M, Mattapallil J, Song K, Tsai WP, Hryniewicz A, Venzon D, Zanetti M, Reimann KA, Roederer M, Franchini G. Reduced protection from simian immunodeficiency virus SIVmac251 infection afforded by memory CD8+ T cells induced by vaccination during CD4+ T-cell deficiency. J Virol. 2008; 82:9629–9638. [PubMed: 18667509]
21. Jin X, Bauer DE, Tuttleton SE, Lewin S, Gettie A, Blanchard J, Irwin CE, Safrit JT, Mittler J, Weinberger L, Kostrikis LG, Zhang L, Perelson AS, Ho DD. Dramatic rise in plasma viremia after CD8(+) T cell depletion in simian immunodeficiency virus-infected macaques. J Exp Med. 1999; 189:991–998. [PubMed: 10075982]
22. Schmitz JE, Kuroda MJ, Santra S, Sasseville VG, Simon MA, Lifton MA, Racz P, Tenner-Racz K, Dalesandro M, Scallon BJ, Ghrayeb J, Forman MA, Montefiori DC, Rieber EP, Letvin NL, Reimann KA. Control of viremia in simian immunodeficiency virus infection by CD8+ lymphocytes. Science. 1999; 283:857–860. [PubMed: 9933172]
23. Matano T, Shibata R, Siemon C, Connors M, Lane HC, Martin MA. Administration of an anti-CD8 monoclonal antibody interferes with the clearance of chimeric simian/human immunodeficiency virus during primary infections of rhesus macaques. J Virol. 1998; 72:164–169. [PubMed: 9420212]
24. Brodie SJ, Lewinsohn DA, Patterson BK, Jiyamapa D, Krieger J, Corey L, Greenberg PD, Riddell SR. In vivo migration and function of transferred HIV-1-specific cytotoxic T cells. Nat Med. 1999; 5:34–41. [PubMed: 9883837]
25. Koenig S, Conley AJ, Brewah YA, Jones GM, Leath S, Boots LJ, Davey V, Pantaleo G, Demarest JF, Carter C, et al. Transfer of HIV-1-specific cytotoxic T lymphocytes to an AIDS patient leads to selection for mutant HIV variants and subsequent disease progression. Nat Med. 1995; 1:330–336. [PubMed: 7585062]
26. Lieberman J, Skolnik PR, Parkerson GR 3rd, Fabry JA, Landry B, Bethel J, Kagan J. Safety of autologous, ex vivo-expanded human immunodeficiency virus (HIV)-specific cytotoxic T-lymphocyte infusion in HIV-infected patients. Blood. 1997; 90:2196–2206. [PubMed: 9310470]
27. Mitsuyasu RT, Anton PA, Deeks SG, Scadden DT, Connick E, Downs MT, Bakker A, Roberts MR, June CH, Jalali S, Lin AA, Pennathur-Das R, Hege KM. Prolonged survival and tissue trafficking following adoptive transfer of CD4zeta gene-modified autologous CD4(+) and CD8(+) T cells in human immunodeficiency virus-infected subjects. Blood. 2000; 96:785–793. [PubMed: 10910888]

28. Kaufmann DE, Lichterfeld M, Altfeld M, Addo MM, Johnston MN, Lee PK, Wagner BS, Kalife ET, Strick D, Rosenberg ES, Walker BD. Limited durability of viral control following treated acute HIV infection. PLoS Med. 2004; 1:e36. [PubMed: 15526059]
29. Autran B, Murphy RL, Costagliola D, Tubiana R, Clotet B, Gatell J, Staszewski S, Wincker N, Assoumou L, El-Habib R, Calvez V, Walker B, Katlama C. Greater viral rebound and reduced time to resume antiretroviral therapy after therapeutic immunization with the ALVAC-HIV vaccine (vCP1452). Aids. 2008; 22:1313–1322. [PubMed: 18580611]
30. Goujard C, Marcellin F, Hendel-Chavez H, Burgard M, Meiffredy V, Venet A, Rouzioux C, Taoufik Y, El Habib R, Beumont-Mauviel M, Aboulker JP, Levy Y, Delfraissy JF. Interruption of antiretroviral therapy initiated during primary HIV-1 infection: impact of a therapeutic vaccination strategy combined with interleukin (IL)-2 compared with IL-2 alone in the ANRS 095 Randomized Study. AIDS Res Hum Retroviruses. 2007; 23:1105–1113. [PubMed: 17919105]
31. Kinloch-de Loes S, Hoen B, Smith DE, Autran B, Lampe FC, Phillips AN, Goh LE, Andersson J, Tsoukas C, Sonnerborg A, Tambussi G, Girard PM, Bloch M, Battegay M, Carter N, El Habib R, Theofan G, Cooper DA, Perrin L. Impact of therapeutic immunization on HIV-1 viremia after discontinuation of antiretroviral therapy initiated during acute infection. J Infect Dis. 2005; 192:607–617. [PubMed: 16028129]
32. Markowitz M, Jin X, Hurley A, Simon V, Ramratnam B, Louie M, Deschenes GR, Ramanathan M Jr. Barsoum S, Vanderhoeven J, He T, Chung C, Murray J, Perelson AS, Zhang L, Ho DD. Discontinuation of antiretroviral therapy commenced early during the course of human immunodeficiency virus type 1 infection, with or without adjunctive vaccination. J Infect Dis. 2002; 186:634–643. [PubMed: 12195350]
33. Schooley RT, Spritzler J, Wang H, Lederman MM, Havlir D, Kuritzkes DR, Pollard R, Battaglia C, Robertson M, Mehrotra D, Casimiro D, Cox K, Schock B. AIDS clinical trials group 5197: a placebo-controlled trial of immunization of HIV-1-infected persons with a replication-deficient adenovirus type 5 vaccine expressing the HIV-1 core protein. J Infect Dis. 2010; 202:705–716. [PubMed: 20662716]
34. Tjernlund A, Zhu J, Laing K, Diem K, McDonald D, Vazquez J, Cao J, Ohlen C, McElrath MJ, Picker LJ, Corey L. In situ detection of Gag-specific CD8+ cells in the GI tract of SIV infected Rhesus macaques. Retrovirology. 2010; 7:1–14. [PubMed: 20078884]
35. Chakrabarti L, Isola P, Cumont MC, Claessens-Maire MA, Hurtrel M, Montagnier L, Hurtrel B. Early stages of simian immunodeficiency virus infection in lymph nodes. Evidence for high viral load and successive populations of target cells. Am J Pathol. 1994; 144:1226–1237. [PubMed: 8203463]
36. Reimann KA, Tenner-Racz K, Racz P, Montefiori DC, Yasutomi Y, Lin W, Ransil BJ, Letvin NL. Immunopathogenic events in acute infection of rhesus monkeys with simian immunodeficiency virus of macaques. J Virol. 1994; 68:2362–2370. [PubMed: 8139022]
37. Okoye A, Park H, Rohankhedkar M, Coyne-Johnson L, Lum R, Walker JM, Planer SL, Legasse AW, Sylwester AW, Piatak M Jr. Lifson JD, Sodora DL, Villinger F, Axthelm MK, Schmitz JE, Picker LJ. Profound CD4+/CCR5+ T cell expansion is induced by CD8+ lymphocyte depletion but does not account for accelerated SIV pathogenesis. J Exp Med. 2009; 206:1575–1588. [PubMed: 19546246]
38. Loffredo JT, Friedrich TC, Leon EJ, Stephany JJ, Rodrigues DS, Spencer SP, Bean AT, Beal DR, Burwitz BJ, Rudersdorf RA, Wallace LT, Piaskowski SM, May GE, Sidney J, Gostick E, Wilson NA, Price DA, Kallas EG, Piontkivska H, Hughes AL, Sette A, Watkins DI. CD8+ T cells from SIV elite controller macaques recognize Mamu-B*08-bound epitopes and select for widespread viral variation. PLoS One. 2007; 2:e1152. [PubMed: 18000532]
39. Loffredo JT, Maxwell J, Qi Y, Glidden CE, Borchardt GJ, Soma T, Bean AT, Beal DR, Wilson NA, Rehrauer WM, Lifson JD, Carrington M, Watkins DI. Mamu-B*08-positive macaques control simian immunodeficiency virus replication. J Virol. 2007; 81:8827–8832. [PubMed: 17537848]
40. Folkvord JM, Anderson DM, Arya J, MaWhinney S, Connick E. Microanatomic relationships between CD8+ cells and HIV-1-producing cells in human lymphoid tissue in vivo. J Acquir Immune Defic Syndr. 2003; 32:469–476. [PubMed: 12679696]

41. Folkvord JM, McCarter MD, Ryder J, Meditz AL, Forster JE, Connick E. alpha-Defensins 1, 2, and 3 are expressed by granulocytes in lymphoid tissues of HIV-1-seropositive and -seronegative individuals. J Acquir Immune Defic Syndr. 2006; 42:529–536. [PubMed: 16837860]
42. Skinner PJ, Daniels MA, Schmidt CS, Jameson SC, Haase AT. Cutting edge: In situ tetramer staining of antigen-specific T cells in tissues. J Immunol. 2000; 165:613–617. [PubMed: 10878330]
43. Allen TM, Sidney J, del Guercio MF, Glickman RL, Lensmeyer GL, Wiebe DA, DeMars R, Pauza CD, Johnson RP, Sette A, Watkins DI. Characterization of the peptide binding motif of a rhesus MHC class I molecule (Mamu-A*01) that binds an immunodominant CTL epitope from simian immunodeficiency virus. J Immunol. 1998; 160:6062–6071. [PubMed: 9637523]
44. Loffredo JT, Sidney J, Bean AT, Beal DR, Bardet W, Wahl A, Hawkins OE, Piaskowski S, Wilson NA, Hildebrand WH, Watkins DI, Sette A. Two MHC class I molecules associated with elite control of immunodeficiency virus replication, Mamu-B*08 and HLA-B*2705, bind peptides with sequence similarity. J Immunol. 2009; 182:7763–7775. [PubMed: 19494300]
45. Loffredo JT, Sidney J, Wojewoda C, Dodds E, Reynolds MR, Napoe G, Mothe BR, O'Connor DH, Wilson NA, Watkins DI, Sette A. Identification of seventeen new simian immunodeficiency virus-derived CD8+ T cell epitopes restricted by the high frequency molecule, Mamu-A*02, and potential escape from CTL recognition. J Immunol. 2004; 173:5064–5076. [PubMed: 15470050]
46. Hardtke S, Ohl L, Forster R. Balanced expression of CXCR5 and CCR7 on follicular T helper cells determines their transient positioning to lymph node follicles and is essential for efficient B-cell help. Blood. 2005; 106:1924–1931. [PubMed: 15899919]
47. Reinhart TA, Rogan MJ, Viglianti GA, Rausch DM, Eiden LE, Haase AT. A new approach to investigating the relationship between productive infection and cytopathicity in vivo. Nat Med. 1997; 3:218–221. [PubMed: 9018242]
48. Li Q, Duan L, Estes JD, Ma ZM, Rourke T, Wang Y, Reilly C, Carlis J, Miller CJ, Haase AT. Peak SIV replication in resting memory CD4+ T cells depletes gut lamina propria CD4+ T cells. Nature. 2005; 434:1148–1152. [PubMed: 15793562]
49. Zhang Z, Schuler T, Zupancic M, Wietgrefe S, Staskus KA, Reimann KA, Reinhart TA, Rogan M, Cavert W, Miller CJ, Veazey RS, Notermans D, Little S, Danner SA, Richman DD, Havlir D, Wong J, Jordan HL, Schacker TW, Racz P, Tenner-Racz K, Letvin NL, Wolinsky S, Haase AT. Sexual transmission and propagation of SIV and HIV in resting and activated CD4+ T cells. Science. 1999; 286:1353–1357. [PubMed: 10558989]
50. Di Mascio M, Paik CH, Carrasquillo JA, Maeng JS, Jang BS, Shin IS, Srinivasula S, Byrum R, Neria A, Kopp W, Catalfamo M, Nishimura Y, Reimann K, Martin M, Lane HC. Noninvasive in vivo imaging of CD4 cells in simian-human immunodeficiency virus (SHIV)-infected nonhuman primates. Blood. 2009; 114:328–337. [PubMed: 19417212]
51. Ganusov VV, De Boer RJ. Do most lymphocytes in humans really reside in the gut? Trends Immunol. 2007; 28:514–518. [PubMed: 17964854]
52. Lay MD, Petravic J, Gordon SN, Engram J, Silvestri G, Davenport MP. Is the gut the major source of virus in early simian immunodeficiency virus infection? J Virol. 2009; 83:7517–7523. [PubMed: 19458001]
53. Petravic J, Vanderford TH, Silvestri G, Davenport M. Estimating the contribution of the gut to plasma viral load in early SIV infection. Retrovirology. 2013; 10:105. [PubMed: 24119218]
54. Vanderford TH, Bleckwehl C, Engram JC, Dunham RM, Klatt NR, Feinberg MB, Garber DA, Betts MR, Silvestri G. Viral CTL escape mutants are generated in lymph nodes and subsequently become fixed in plasma and rectal mucosa during acute SIV infection of macaques. PLoS pathogens. 2011; 7:e1002048. [PubMed: 21625590]
55. Mattapallil JJ, Douek DC, Hill B, Nishimura Y, Martin M, Roederer M. Massive infection and loss of memory CD4+ T cells in multiple tissues during acute SIV infection. Nature. 2005; 434:1093–1097. [PubMed: 15793563]
56. Stahl-Hennig C, Eisenblatter M, Franz M, Stoiber H, Tenner-Racz K, Suh YS, Jasny E, Falkensammer B, Ugucchioni M, Georgsson G, Baroni C, Dierich MP, Lifson JD, Steinman RM, Uberla K, Racz P, Ignatius R. A single vaccination with attenuated SIVmac 239 via the tonsillar route confers partial protection against challenge with SIVmac 251 at a distant mucosal site, the rectum. Front Biosci. 2007; 12:2107–2123. [PubMed: 17127448]

57. Minang JT, Trivett MT, Coren LV, Barsov EV, Piatak M Jr. Ott DE, Ohlen C. Nef-mediated MHC class I down-regulation unmasks clonal differences in virus suppression by SIV-specific CD8(+) T cells independent of IFN-gamma and CD107a responses. Virology. 2009; 391:130–139. [PubMed: 19555986]

58. Kim CH, Rott LS, Clark-Lewis I, Campbell DJ, Wu L, Butcher EC. Subspecialization of CXCR5+ T cells: B helper activity is focused in a germinal center-localized subset of CXCR5+ T cells. J Exp Med. 2001; 193:1373–1381. [PubMed: 11413192]

59. Elahi S, Niki T, Hirashima M, Horton H. Galectin-9 binding to Tim-3 renders activated human CD4+ T cells less susceptible to HIV-1 infection. Blood. 2012; 119:4192–4204. [PubMed: 22438246]

60. Cubas RA, Mudd JC, Savoye AL, Perreau M, van Grevenynghe J, Metcalf T, Connick E, Meditz A, Freeman GJ, Abesada-Terk G Jr. Jacobson JM, Brooks AD, Crotty S, Estes JD, Pantaleo G, Lederman MM, Haddad EK. Inadequate T follicular cell help impairs B cell immunity during HIV infection. Nat Med. 2013; 19:494–499. [PubMed: 23475201]

61. Hofmeyer KA, Jeon H, Zang X. The PD-1/PD-L1 (B7-H1) pathway in chronic infection-induced cytotoxic T lymphocyte exhaustion. Journal of biomedicine & biotechnology. 2011; 2011:451694. [PubMed: 21960736]

62. Fukazawa Y, Park H, Cameron MJ, Lefebvre F, Lum R, Coombes N, Mahyari E, Hagen SI, Bae JY, Iii MD, Swanson T, Legasse AW, Sylwester A, Hansen SG, Smith AT, Stafova P, Shoemaker R, Li Y, Oswald K, Axthelm MK, McDermott A, Ferrari G, Montefiori DC, Edlefsen PT, Piatak M Jr. Lifson JD, Sekaly RP, Picker LJ. Lymph node T cell responses predict the efficacy of live attenuated SIV vaccines. Nat Med. 2012; 18:1673–1681. [PubMed: 22961108]

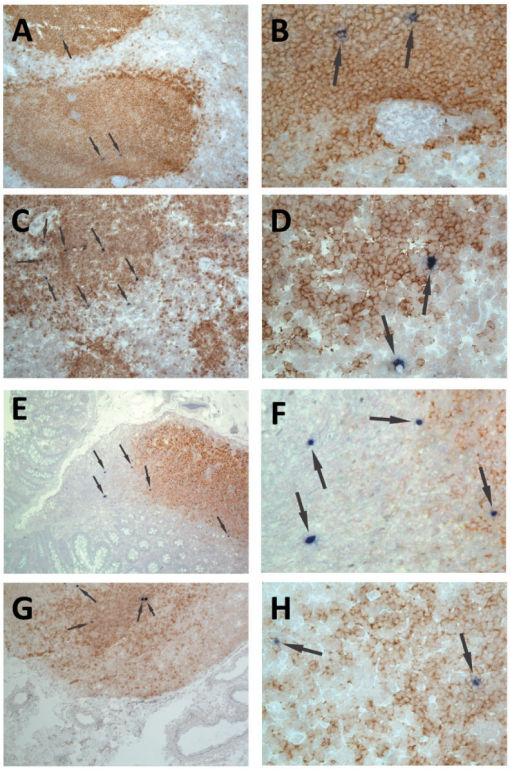


**Figure 1. Localization of SIV RNA+ cells in secondary lymphoid tissues of chronically infected rhesus macaques**

Representative images of *in situ* hybridization for SIV RNA to identify virus-producing cells (blue/black cells indicated by arrows) and CD20 staining (brown) to morphologically identify B cell follicles in spleen (A, B), axillary lymph node (C, D), ileum (E, F) and colon (G, H). Images B, D, F and H are high magnification (original magnification 252X) images from the fields shown in A, C, E and F (original magnification 63X), respectively.

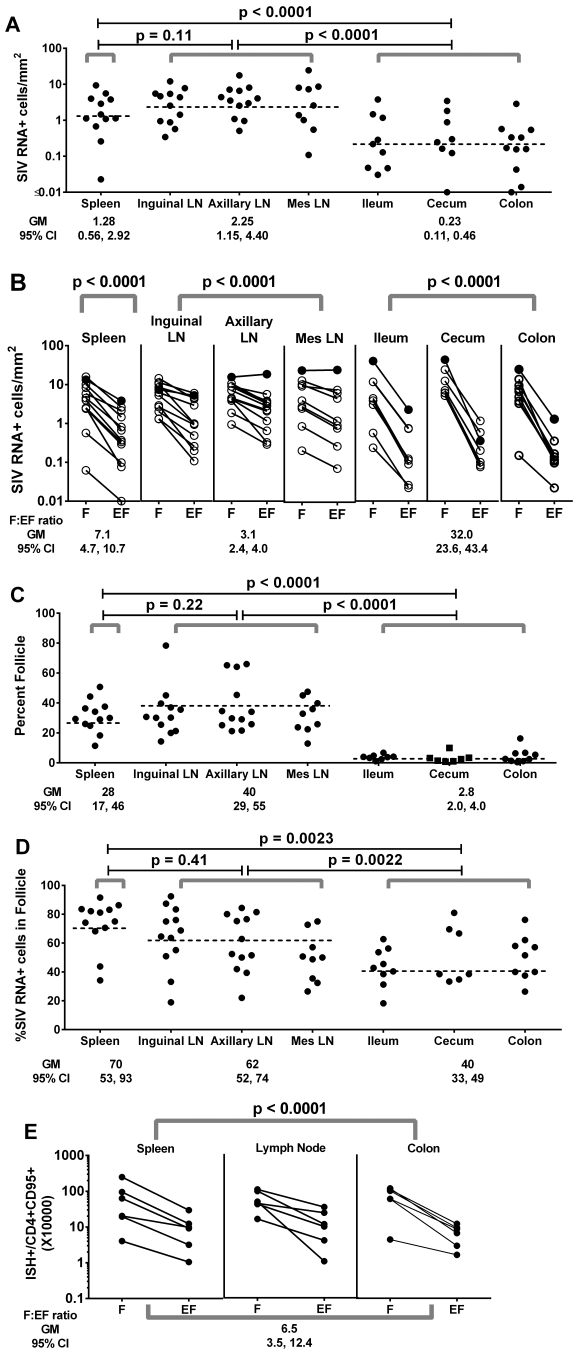


**Figure 2. Distribution of SIV RNA+ cells in secondary lymphoid tissue compartments of chronically SIV-infected rhesus macaques**

(A) Frequencies of total SIV RNA+ cells differed among secondary lymphoid tissues ($p<0.0001$). (B) Frequencies of SIV RNA+ cells in B-cell follicles (indicated by F) and extrafollicular regions (indicated as EF) differed among lymphoid tissues ($p<0.0001$). (C) Percentages of secondary lymphoid tissues constituted by B cell follicles differed among lymphoid tissues ($p<0.0001$). (D) Percentages of SIV RNA+ cells located in B cell follicles differed among lymphoid tissues ($p=0.0005$). (E) Frequencies of SIV RNA+ cells in B-cell follicles were significantly higher than those in extrafollicular regions ($P<0.0001$), after

adjusting for frequencies of CD95+CD4+ cells in each compartment (Supplemental Figure 1C). There were no differences in the F:EF ratio among tissues ($p=0.67$) nor were there differences in levels of SIV-producing cells in these compartments among tissues ($p>0.51$) after adjusting for CD95+CD4+ cells. Data were analyzed using a model that controlled for multiple observations within the same animal for each type of lymphoid tissue, indicated by gray brackets. Dotted horizontal lines indicate the geometric mean (GM) within the model for each type of tissue, which is also shown in the data below each graph. LN indicates lymph node. Mes indicates mesenteric.

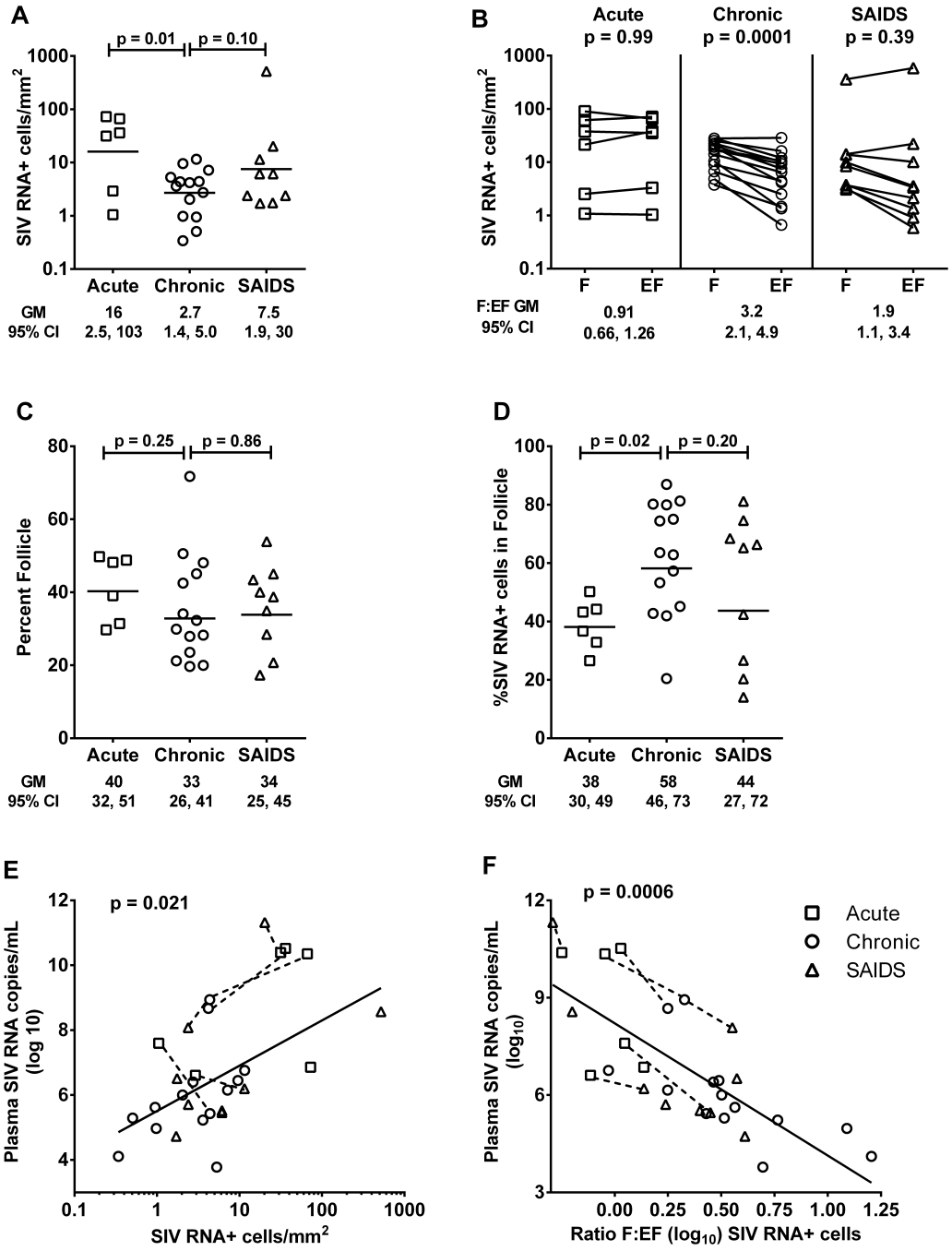


**Figure 3. Distribution and frequency of SIV RNA+ cells in lymph nodes of rhesus macaques during acute infection (day 14), chronic asymptomatic infection, and simian AIDS (SAIDS)**

(A) Frequencies of SIV RNA+ cells in lymph nodes. (B) Frequencies of SIV RNA+ cells in B cell follicles (F) compared to extrafollicular regions (EF) of lymph nodes. (C) Percentage of tissue that consisted of follicle did not differ among animals by disease stage. (D) Percentages of SIV RNA+ cells within B cell follicles. (E) Frequencies of SIV RNA+ cells within lymph nodes predicted plasma viral load. For every 1 $\log_{10}$ increase in SIV RNA+ cells, there was a 1.40 $\log_{10}$ (95% CI, 0.35, 2.45) increase in plasma viral load. (F) The F:EF ratio of SIV RNA+ cells in lymph nodes predicted plasma viral load. On average, viral load

decreased by 4.0 $\log_{10}$ (95% CI, −5.33, −2.67) copies/mL for each 1 $\log_{10}$ increase in F:EF. This relationship did not significantly differ by disease stage (p=0.30). Furthermore, when the analysis was restricted to animals with chronic, asymptomatic infection, results were still statistically significant (p=0.0078), with viral load decreases by 3.04 $\log_{10}$ (95%CI −5.12, −0.96) copies/mL for each 1 $\log_{10}$ increase in F:EF. Dotted lines link data points from animals that were sampled in more than one disease stage. Horizontal lines indicate geometric mean (GM) values.

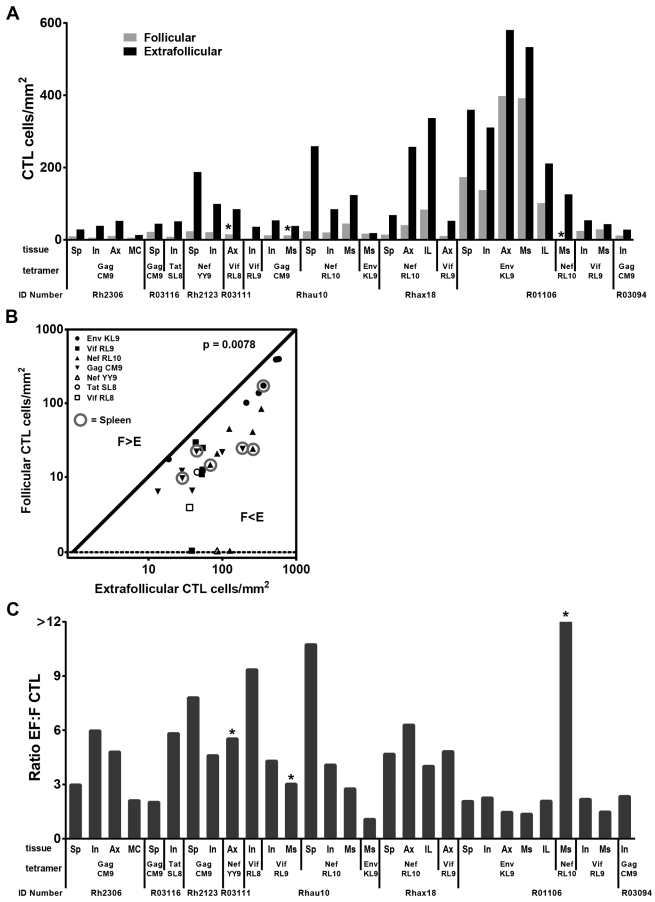


**Figure 4. Quantification of SIV-specific CTL in compartments of lymph node (LN) and spleen (Sp) from chronically infected rhesus macaques**

(A) Frequencies of SIV-specific CTL in follicular and extrafollicular compartments according to animal and CTL epitope. Frequencies of virus-specific CTL were significantly higher (p=0.0078) in extrafollicular regions compared to follicular regions in both lymph node (medians, 54 cells/mm$^2$ versus 17 cells/mm$^2$, respectively) and spleen (medians, 128 cells/mm$^2$ versus 23 cells/mm$^2$, respectively), using an exact binomial test in which results for each animal were collapsed. (B) Relationship between frequencies of extrafollicular and follicular SIV-specific CTL. Samples from spleen are indicated with a circle, whereas all others are from lymph node. Extrafollicular SIV-specific CTL was a significant predictor of follicular CTL (p=0.0024). For every 1 $\log_{10}$ increase in extrafollicular SIV-specific CTL, there was on average a 0.72 $\log_{10}$ (95% CI, 0.30, 1.14) increase in follicular CTL. (C) Ratio of extrafollicular (EF) to follicular (F) SIV-specific CTL. *indicates animals who had no SIV-specific CTL detected in folliclesIn these cases, a value of 1 cell per total tissue area evaluated was assigned. For animal R01106, the EF:F Nef RL10-specific CTL ratio was 54. Abbreviations: Sp=spleen; In=inguinal lymph node; Ax=axillary lymph node; Il=iliac lymph node; MC=mesocolonic lymph node; Ms=mesenteric lymph node.

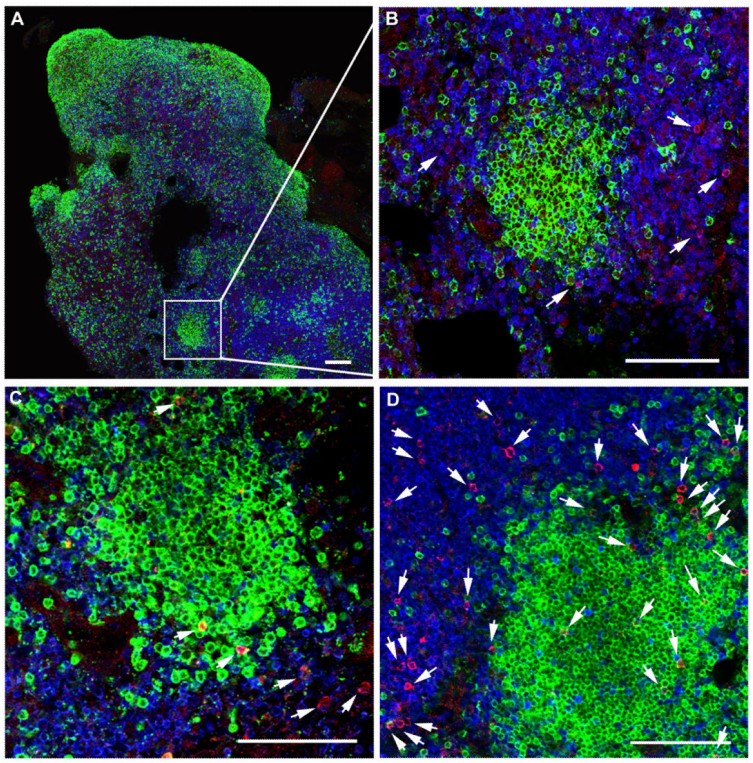


**Figure 5. Localization of SIV-specific CTL in secondary lymphoid tissues of rhesus macaques during chronic infection**

Representative lymph node tissue sections stained with MHC class I tetramers (red) to label SIV-specific CTL, CD3 antibodies (blue) to label T cells, and CD20 antibodies (green) to label B cells and delineate B cell follicles. (A) Shows a montage of multiple confocal projected z-scans from an inguinal lymph node from animal Rhau10 stained with Mamu-B*008:01/Vif RL8 tetramers. (B-D) are confocal z-scans showing the range of localization patterns of SIV-specific CTL within follicles typically seen in spleen and lymph nodes from animals in the study. (B) Enlargement from A demonstrating a B cell follicle devoid of CTL. (C) Tissue section from the same lymph node shown in A and B now stained with Mamu-B*008:01/Vif RL9 tetramers demonstrating an example of CTL located on the follicle edge. (D) A mesocolonic lymph node section from animal R03116 stained with Mamu-A*001:01/Gag CM9 tetramers exemplifying CTL distributed throughout a follicle. Tetramer + cells within the sections were identified in montages of high-resolution serial z-scans, and are indicated by arrows in B-D. Within individual z-scans, tops and bottoms of cells were distinguished from non-specific background staining by stepping up and down through the adjacent z-scans. Red staining in the images without arrows was determined to be background staining by this technique. Confocal images were collected with a 20X objective and each scale bar indicates 100 μm.

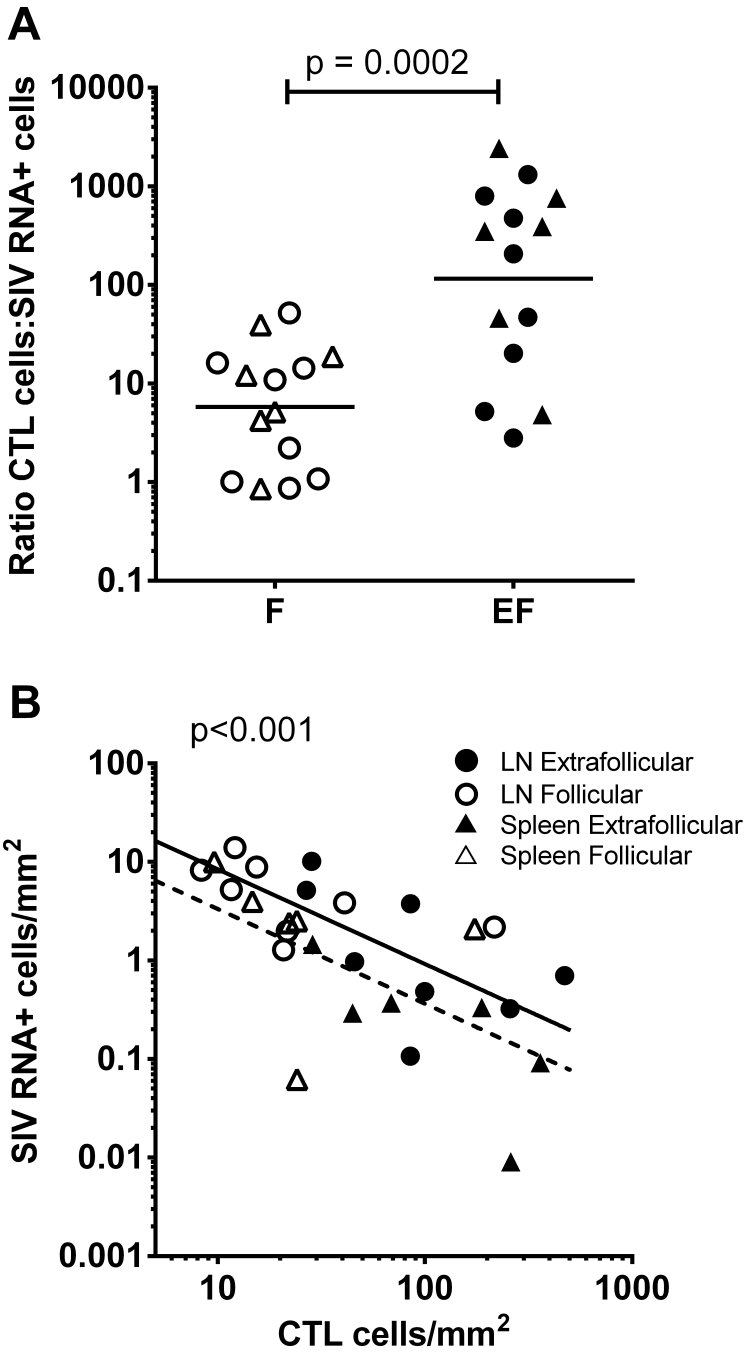


**Figure 6. *In vivo* relationships between SIV-specific CTL and SIV RNA+ cells within compartments of lymph node (LN) and spleen from chronically infected rhesus macaques**

(A) Effector to target cell ratios of SIV-specific CTL to SIV RNA+ cells were significantly higher in extrafollicular (EF) compared to follicular compartments (F) for both lymph node (n=8) and spleen (n=6). (B) Frequencies of SIV-specific CTL within F and EF predicted frequencies of SIV RNA+ cells within those compartments in a mixed model analysis that controlled for tissue type. For every 1 $\log_{10}$ increase in SIV-specific CTL, there was on average a −0.96 change in $\log_{10}$ SIV RNA+ cells (95% CI, −1.31,−0.61). Results for spleen are summarized by the dotted line and for lymph node by the solid line. If data were

available for more than one CTL epitope in an animal, only the most abundant SIV-specific CTL response was evaluated. If data were available for multiple lymph nodes in an animal, results were averaged.

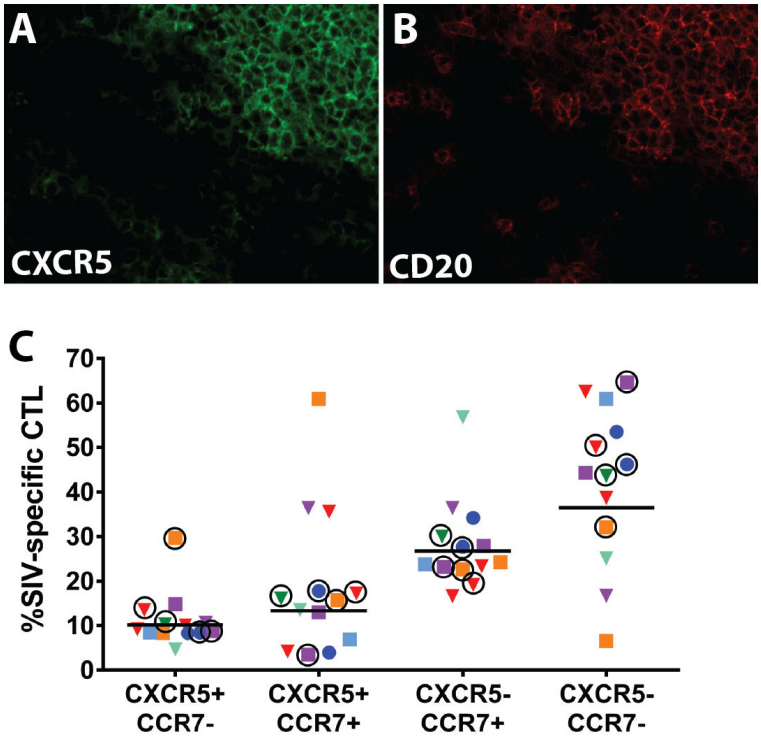


**Figure 7. CXCR5 expression within lymph node and spleen of chronically SIV_infected rhesus macaques and on SIV-specific CTL**

(A,B) Representative images of a double-stained spleen section from animal Rh2123 demonstrating that most CXCR5+ cells shown in green (A) are localized within B cell follicles defined by CD20 staining and shown in red (B). (C) Percentages of subsets of SIV-specific cells defined by CXCR5 and CCR7 expression from lymph nodes and spleens of SIV-infected rhesus macaques as determined by flow cytometry (see gating strategy in Supplemental Figure 3). Each animal is indicated by a different color. Triangles indicate CTL directed against SIV Gag CM9, circles indicate CTL directed against Nef YY9, and squares indicate CTL directed against Nef RL10. Spleen tissues are indicated by a circle around the symbol and symbols without a circle around them indicate lymph node cells. Results for spleen and lymph node were not statistically different (p=0.30). Horizontal lines indicate the geometric mean.

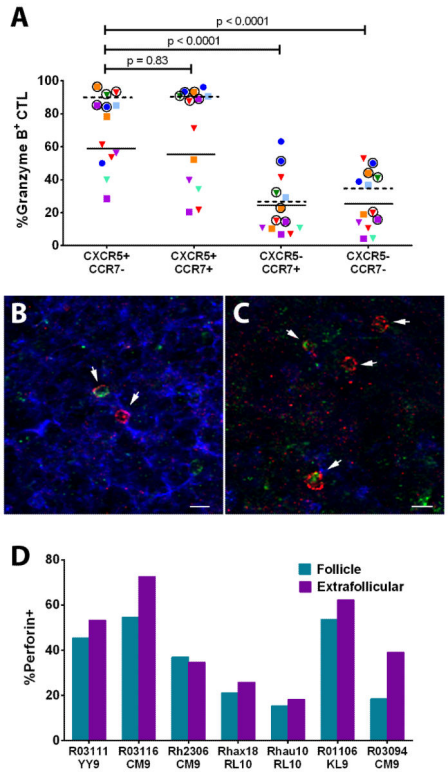


**Figure 8. CTL effector protein expression within follicular and extrafollicular SIV-specific CTL in spleen and lymph nodes of rhesus macaques**

(A) Granzyme B expression within follicular (CXCR5+CCR7-) and extrafollicular (CXCR5- and/or CCR7+) subsets of SIV-specific CTL as determined by tetramer staining and flow cytometry (see gating strategy in Supplemental Figure 3). Each animal is indicated by a different color. Triangles indicate CTL directed against SIV Gag CM9, circles indicate CTL directed against Nef YY9, and squares indicate CTL directed against Nef RL10. Spleen tissues are indicated by a circle around the symbol and symbols without a circle around them indicate lymph node cells. Granzyme B expression was significantly higher in spleen (horizontal dotted lines indicates mean values) compared to lymph node (horizontal solid lines indicate mean values) ($p<0.0001$). (B, C) Representative images of *in situ* perforin staining within SIV-specific CTL located in follicular (B) and extrafollicular (C) regions of a lymph node from animal Rh2306 stained with Mamu-A*001:01/Gag CM9 tetramers (red), anti-perforin antibodies (green), and anti-IgM (blue) to define B-cell follicles morphologically. Confocal z-scans were collected with a 20X objective. Scale bar in B is 50 μm and in C is10 μm. (D) Percentages of perforin+ tetramer-binding cells within and outside of lymph node follicles determined by *in situ* staining. Using a generalized linear model for a negative binomial distribution that accounted for within subjects correlation and adjusted for $\log_e$ (area), the percentage of perforin+ cells within the tetramer-binding population was approximately 15.9% (95% CI, 8.6%, 22.6%) lower in follicles compared to extrafollicular regions ($p<0.001$).

## Table 1

Clinical and Experimental Characteristics of Rhesus Macaques

| | ID Number[a] | Weeks post Infection | Plasma SIV RNA ($log_{10}$ copies/mL) | CD4+ T cell count (cells/$mm^3$) | Route of infection[b] | MHC class I alleles |
|---|---|---|---|---|---|---|
| Acute | 2H2 | 2 | 10.35 | 822 | IV | [c] |
| | 0H7 | 2 | 10.39 | 1436 | IV | [c] |
| | 8G5 | 2 | 10.52 | 1063 | IV | [c] |
| | r03094 | 2 | 6.61 | 394 | R | [c] |
| | 4440 | 2 | 7.60 | 1736 | IV | [c] |
| | 28827 | 2 | 6.86 | [d] | V | [c] |
| Chronic | Rh2284-N | 12 | 6.40 | 374 | R | [c] |
| | Rh2306-N | 12 | 6.15 | 291 | R | A01, A02, B01 |
| | R03116-N | 23 | 3.78 | 422 | R | A01 |
| | R03103-N | 16 | 5.23 | 317 | R | [c] |
| | R03141-N | 16 | 6.00 | 324 | R | [c] |
| | 2H2 | 36 | 8.94 | 1408 | IV | [c] |
| | 8G5-N | 43 | 8.67 | 1221 | IV | [c] |
| | Rh2123-N | 56 | 5.62 | [d] | IV | A01, B30 |
| | R02017-N | 88 | 5.29 | [d] | IV | [c] |
| | R02076-N | 16 | 6.76 | 315 | IV | [c] |
| | R03111-N | 15 | 6.45 | 362 | R | A02 |
| | Rhau10-N | 241 | 4.11 | 569 | IV | B08 |
| | Rhaxl8-N | 78 | 4.97 | 334 | R | B08 |
| | 4440 | 20 | 5.43 | 2099 | IV | [c] |
| SAIDS[e] | Rhav84 | 28 | 5.52 | 45 | IV | [c] |
| | Rhav77 | 28 | 5.71 | 123 | IV | [c] |
| | R03094 | 22 | 6.20 | 194 | R | A01 |
| | 0H7-N | 20 | 11.32[f] | 950 | IV | [c] |
| | 2H2-N | 44 | 8.08 | 92 | IV | [c] |
| | R97009 | 26 | 8.57 | 158 | R | [c] |
| | R98019 | 22 | 6.51 | 489 | R | [c] |
| | R01106-N | 81 | 4.73 | 142 | R | B08 |
| | Rhaj10 | 26 | 5.46 | 53[g] | R | [c] |

[a] Numbers that are followed by the letter “N” indicate animals who were euthanized and from which lymph nodes, spleen and GALT were obtained at necropsy.

[b] Abbreviations for route of SIV infection: IV, intravenous, R, intra-rectal, V, intravaginal.

[c] In situ tetramer staining not performed on this animal on this date.

[d] Test not done.

[e] Simian AIDS (SAIDS) was defined as an animal that had <200 CD4+ T cells/$mm^3$ and/or a SAIDS defining illness.

[f] Viral load was performed one week prior to this time point.

[g] CD4+ T cell count was performed 3 months prior to this time point.